Available online at www.sciencedirect.com
ScienceDirect
Polymer 48 (2007) 1360–1366
polymer
www.elsevier.com/locate/polymer

Experimental studies and molecular modelling of the stress–optical and stress–strain behaviour of poly(ethylene terephthalate). Part I: Infra-red spectroscopic investigation and modelling of chain conformation and orientation changes on drawing

L.S. Saunders [a], I.M. Ward [a,*], J.I. Cail [b], R.F.T. Stepto [b]

[a] *IRC in Polymer Science and Technology, School of Physics and Astronomy, University of Leeds, Leeds LS2 9JT, UK*
[b] *Polymer Science and Technology Group, School of Materials, The University of Manchester, Grosvenor Street, Manchester M1 7HS, UK*

Received 9 September 2006; received in revised form 20 December 2006; accepted 31 December 2006
Available online 26 January 2007

Abstract

Quantitative infra-red data on oriented poly(ethylene terephthalate) (PET) films have been used to determine the changes in the proportions of the *trans* and *gauche* conformers of the glycol residues and the development of molecular orientation of the terephthaloyl groups as functions of draw ratio. The results are compared with predictions for the stretching of a rubber-like network based on rotational-isomeric-state (RIS) Monte Carlo (MC) modelling. It is shown that both sets of data are consistent with stretching an entangled molecular network of about 10 PET monomer units per network chain. The onset of crystallisation at a draw ratio of 2.5 affects the glycol *trans–gauche* conformer contents but has no detectable effect on terephthaloyl orientation.

Keywords: Infra-red; Poly(ethylene terephthalate); Monte-Carlo modelling

1. Introduction

This paper is one of a series of publications addressing the modelling of the development of molecular orientation in poly(ethylene terephthalate) (PET). It is well established that the starting point for such modelling is that the orientation process can be regarded as stretching the rubber-like network that exists above T_g, either in a melt spinning or a hot-drawing process [1,2]. The molecular orientation has been quantified by the stress–optical behaviour [1] or by measurements of molecular orientation using a range of experimental techniques including infra-red and Raman spectroscopy [3,4], polarized fluorescence [5] and NMR [6]. In all cases, it has been usual to interpret the data in terms of the Kuhn and Grün theory [7], originally proposed for the stress–optical behaviour of rubber networks. This theory replaces the true network by an idealised network of chains, each chain containing a number of freely-jointed links, and each link consisting of several monomer units. Although the Kuhn and Grün theory has provided a quantitative phenomenological basis for relating degrees of molecular orientation measured by spectroscopic methods and refractive index measurements to macroscopic stretch ratios, it does not provide quantitative understanding at the molecular level.

With the development by Stepto and co-workers of a Monte Carlo (MC) approach using rotational-isomeric-state (RIS) models of the network chains [8–10], it has now been possible to revisit this area of research and make precise quantitative predictions of the stress–strain behaviour and the development of molecular orientation. In one of our previous papers, the use of stress–optical measurements to characterise oriented PET was reviewed [11] and a preliminary account of

* Corresponding author. Tel.: +44 113 343 3808; fax: +44 113 343 3846.
E-mail address: i.m.ward@leeds.ac.uk (I.M. Ward).

0032-3861/$ - see front matter © 2007 Elsevier Ltd. All rights reserved.
doi:10.1016/j.polymer.2006.12.048

attempts to apply the MC method of Stepto et al. was given. This early work is now being superseded by more detailed studies and the work so far has been published in three recent papers. First, it was necessary to modify the original Williams–Flory RIS model for PET to match characteristic ratios $\left(\langle r^2\rangle/M\right)$ in the melt measured by neutron scattering and the *trans–gauche* conformation populations of the glycol segments, measured by infra-red spectroscopy [12,13]. Secondly, the MC method was developed to model the stress–strain behaviour of PET networks [14]. These papers provide the basis for the further developments to model stress–optical behaviour and spectroscopic measurements of molecular orientation. It has been decided to proceed in two stages. First, in this paper we show how the infra-red measurements of the conformational changes and molecular orientation can be understood quantitatively using the MC modelling. Secondly, in the next two papers, armed with this infra-red data, the development of birefringence with deformation will be predicted and compared with experimental measurements. From the totality of stress–strain measurements, infra-red and optical measurements it is then possible to obtain a quantitative interpretation of the stress–optical behaviour and replace the phenomenological Kuhn and Grün theory by a quantitative treatment based on detailed molecular understanding.

2. Experimental techniques

2.1. Determination of molecular weight

A melt extruded isotropic PET sheet of thickness 30 μm was supplied by DuPont UK Ltd. The temperature of the extruded melt was in the range of 533–553 K [15]. The number average molecular weight, M_n, of the isotropic PET film was determined by measurement of the intrinsic viscosity. Small pieces of the film were dried in a vacuum oven at 80 °C for 16 h. A small amount of the film was then weighed and dissolved in *o*-chlorophenol, and left to equilibrate at 25 °C. The intrinsic viscosity at this temperature was determined using a dilution series in an Ubbelohde viscometer and found to be 0.62 dL g^{-1}.

Ravens and Ward [16] have shown that for PET dissolved in *o*-chlorophenol the intrinsic viscosity at 25 °C is related to the number average molecular weight, M_n, by

$$\left[\eta\right] = 1.7 \times 10^{-4} M_n^{0.83}. \quad (1)$$

The number average molecular weight of the PET sample studied here was hence calculated to be 19,500.

2.2. Drawn sample preparation

Dumbbell shaped samples with a gauge length of 60 mm were cut from the sheet with a scalpel using a steel template, and lines drawn across the gauge at 1 cm intervals. The dumbbells were then extended for a few seconds in an Instron tensile testing machine at 85 °C, using a nominal strain rate of 5 min^{-1}. Immediately after drawing, and while still held at full extension in the machine grips, the samples were quenched using a can of freezer spray. The final draw ratios and the uniformity of the deformations were determined from the new spacings of the ruled lines. A series of samples with a range of draw ratios up to 4.3:1 were thus produced. The draw ratio is equal to the uniaxial deformation ratio, λ.

The densities of the isotropic and drawn materials at 298 K were determined using a potassium iodide density-gradient column.

2.3. Refractive index measurements

An Abbé refractometer was used to measure the refractive indices, n_j, of the PET film in three perpendicular directions; $j = 1$ corresponds to measurement in the plane of the film, perpendicular to the draw direction, $j = 2$ to measurement through the thickness of the film and $j = 3$ corresponds to measurement parallel to the draw direction.

2.4. Infra-red spectroscopy

The three skeletal bonds of the glycol segment of the PET repeat unit (3–4, 4–5, 5–6 in Fig. 1(a)–(c)) may exist in either the *trans* conformation or a *gauche* conformation, with the proportion of *trans* conformations increasing with the draw ratio as the chains extend. Infra-red spectroscopy

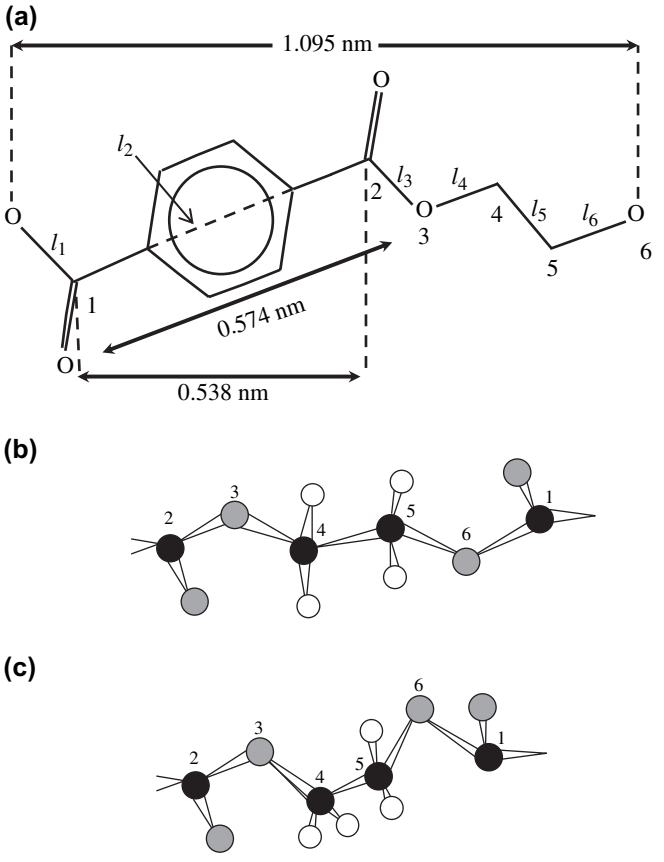

Fig. 1. (a) PET repeat unit in the fully-extended all-*trans* conformation, and the glycol segment in the (b) *trans* and (c) *gauche* conformations.

has been used to quantify this change, as well as to measure the increase in the orientation of the terephthaloyl residue with draw ratio.

The infra-red absorbance spectra of the drawn samples were determined using a single beam BOMEM FTIR spectrometer. In each experiment 100 spectra were recorded over the wavenumber range 500–1150 cm^{-1} and then averaged. A KR-202 wire-grid polarizer was used to polarize the radiation and hence to measure for each PET sample the absorbance of radiation both parallel with and perpendicular to the draw direction. The principal direction of the polarizer was set at 45° to the vertical in order to eliminate the effects of any inherent beam polarization. The spectra were compared to a reference spectrum obtained when the spectrometer was run with no sample in place to give the parallel and perpendicular measured absorbances A_3 and A_1. An example of a FTIR absorbance spectrum for PET is shown in Fig. 2.

The initial positions of the peaks were chosen using the values quoted by previous workers in this laboratory [17–19]. To calculate the true absorbances of the drawn samples, a series of corrections were applied to the data as described in detail in a previous publication [13]. Briefly, a baseline correction was made and then the data were corrected for the effects of imperfect polarizers [20]. Thermo Galactic software [21] was then used to generate a theoretical spectrum consisting of 41 individual peaks, with three new peaks being added at the high wavenumber end of the spectrum in order to fit the tail of the data.

The position and halfwidth of each peak were allowed to vary by a few wavenumbers, and the height of each was initially left unrestrained. The shape of each peak was allowed to vary between a Gaussian and a Lorentzian curve. A minimisation process then fitted the master theoretical curve to those for the drawn samples, producing values of the position, the height and the area of each constituent peak.

The areas under the peaks of interest were then corrected to account for reflections from the sample surface and the thickness of the sample [22] to give values of k_j:

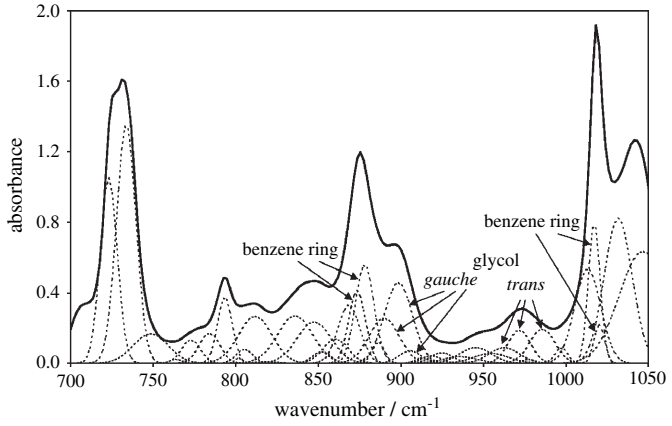

Fig. 2. An infra-red absorption spectrum for PET showing the key bands studied in this work. The experimentally measured curve is shown, together with the individually calculated constituent peaks.

$$k_j = \frac{A_j \lambda}{0.4343 \times 4 \times \pi \times t}, \tag{2}$$

where λ is the wavenumber, t is the sample thickness and j is 1 or 3 as before. The values of k_j were then corrected for the internal field, using the refractive index values, n_j, to calculate values ϕ_j proportional to the imaginary part of the average complex principal polarizability. The quantity $\phi_j = (4/3)\pi N\langle\alpha_j''\rangle$, where N is the concentration of absorbing species per unit volume and $\langle\alpha_j''\rangle$ is the imaginary part of the average complex principal polarizability, is given for small absorbances to a good approximation by

$$\phi_j = \frac{6 n_j k_j}{(n_j + 2)^2}. \tag{3}$$

For uniaxially drawn materials, the orientation is assumed to be transversely isotropic and so the polymeric chains are assumed to have no preferred orientation in directions perpendicular to the draw direction. Therefore $\phi_1 = \phi_2$ and so the average value ϕ_{av} at a particular wavenumber is given by

$$\phi_{av} = \frac{1}{3}(\phi_3 + 2\phi_1). \tag{4}$$

2.4.1. Gauche content of glycol segment

Vibrations of the *trans* and *gauche* conformers of the glycol segment give rise to absorbance peaks at 963, 972 and 978 cm^{-1}, and 890, 899 and 906 cm^{-1}, respectively [23–25]. The infra-red extinction coefficients for the *trans* and *gauche* conformers are known to be equal. The proportion of segments in the *gauche* state may therefore be determined from the ratio of the sum of the values of ϕ_{av} measured at the latter three wavenumbers to the sum of the values for all six glycol bands:

$$\%\ gauche\ \text{conformers} = \frac{\sum \phi_{av}(gauche)}{\sum \phi_{av}(gauche) + \sum \phi_{av}(trans)} \times 100. \tag{5}$$

Finally, determination of the *% gauche* conformers of the drawn samples allows the *gauche* content to be determined as a function of draw ratio.

2.4.2. Terephthaloyl orientation

To determine the orientation of the terephthaloyl groups, two pairs of infra-red absorption bands associated with benzene ring vibrations were chosen for which the directions of the transition moment vectors are well known. The bands are at 873 and 878 cm^{-1}, and 1017 and 1021 cm^{-1}. The assignment of these bands is due to Ward and co-workers [23–26] and Boerio et al. [27]. As shown in Fig. 3(a), the vibrations giving rise to the peaks at 1017 and 1021 cm^{-1} are in-plane C–H deformation vibrations which have their transition moments along the 1–2 direction, corresponding to the terephthaloyl segment vector. The vibrations giving rise to the peaks at 873 and 878 cm^{-1} are out-of-plane C–H

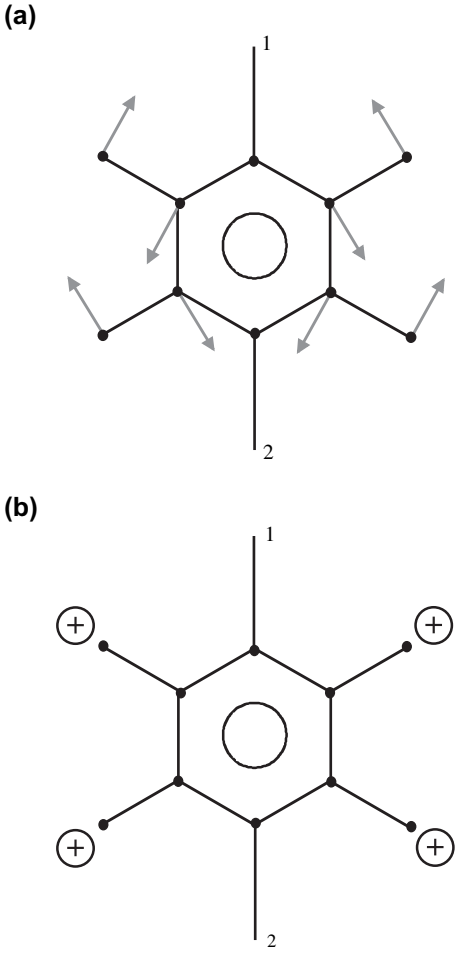

Fig. 3. Vibration modes of the benzene ring. (a) In-plane C–H vibrations, giving rise to absorbance peaks at 1017 and 1021 cm^{-1}. (b) Out-of-plane C–H vibrations, giving rise to absorbance peaks at 873 and 878 cm^{-1}.

deformation vibrations which have their transition moment vectors normal to the plane of the benzene ring, as in Fig. 3(b).

For transversely isotropic materials the terephthaloyl orientation can be defined in terms of the average angle, ζ, that the segments make with the draw direction, as shown in Fig. 4. The average orientation function $\langle P_2(\cos\zeta_{ter})\rangle$ is given by

$$\langle P_2(\cos\zeta_{ter})\rangle = \frac{1}{2}\left(3\langle\cos^2\zeta_{ter}\rangle - 1\right). \quad (6)$$

If it is assumed that there is no preferred orientation of the segmental transition moment vectors in directions perpendicular to the segment axis, and that the angle between the segmental transition moment vector and the draw direction γ, the orientation average $\langle P_2(\cos\gamma)\rangle$ is obtained from

$$\langle P_2(\cos\gamma)\rangle = \frac{(\phi_3-\phi_1)}{(\phi_3+2\phi_1)}, \quad (7)$$

and $\langle P_2(\cos\zeta_{ter})\rangle$ is evaluated from

$$\langle P_2(\cos\zeta_{ter})\rangle P_2(\cos\delta) = \langle P_2(\cos\gamma)\rangle, \quad (8)$$

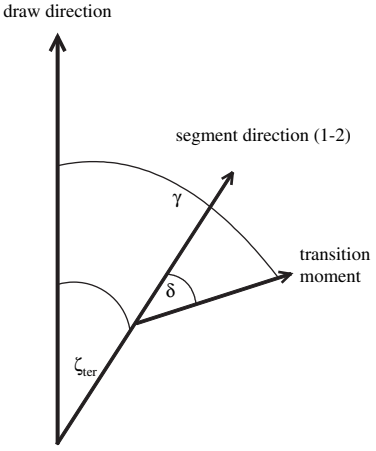

Fig. 4. Definition of orientation angles used in infra-red measurements of the terephthaloyl segments.

where δ is the angle between the segment axis and the segmental transition moment vector.

For the 1021 and 1017 cm^{-1} peaks $P_2(\cos\delta) = 1$, and hence the average orientation measured from the dichroism of these bands, $\langle P_2(\cos\gamma)\rangle_{1017,1021}$ is given by

$$\langle P_2(\cos\zeta_{ter})\rangle = \langle P_2(\cos\gamma)\rangle_{1017,1021}, \quad (9)$$

i.e., the segment axis orientation relative to the draw direction can be found directly from the infra-red measurements. The 873 and 878 cm^{-1} bands correspond to vibrations perpendicular to the segment direction, so $\delta = 90°$ and $P_2(\cos\delta) = -0.5$. Hence,

$$\langle P_2(\cos\zeta_{ter})\rangle = -2\langle P_2(\cos\gamma)\rangle_{873,878}. \quad (10)$$

Further,

$$\langle P_2(\cos\gamma)\rangle_{1017,1021} = -2\langle P_2(\cos\gamma)\rangle_{873,878}. \quad (11)$$

The infra-red spectroscopy measurements performed here allow us to measure directly $\langle P_2(\cos\gamma)\rangle_{1017,1021}$ and $\langle P_2(\cos\gamma)\rangle_{873,878}$ and therefore to test the validity of the relationship in Eq. (11).

3. Modelling

3.1. Network MC calculations

In the MC algorithm, a network of polymer chains is represented by an array of individual RIS chains, initially randomly oriented in three dimensions. The chains are generated bond-by-bond, using conditional conformational probabilities and Metropolis sampling, to give a population of end-to-end distances, r, distributed according to their radial distribution function, $W(r)$. Each chain is deformed uniaxially, assuming affine chain deformation up to a maximum extension [8–10]. The application of the network MC calculations to PET has been described previously [13,14]. The simulations were performed for a range of values of n, the number of repeat units per chain,

i.e. in PET melts, the length of chains between entanglements. Matching experimental values of $(\langle r^2\rangle/M)_\infty$ for melts at 523 K and the proportion of *gauche* glycol conformers showed that a new rotational-isomeric-state (RIS) model of the PET chain was needed. The depth of the *gauche* minimum around the C–C bond of the O–C–C–O sequence in the glycol unit, $E_{\sigma 5}$, was increased to -4.16 kJ mol^{-1} and all other energy and geometrical parameters were as specified in the Williams–Flory model [28] for PET chains in solution. The details are given in the following paper (Part II) [29].

3.2. Proportion of gauche glycol conformers

MC calculations performed on the RIS model for PET [13,14] were used to simulate uniaxial deformation of the network. Predictions of the variation of the proportion of *gauche* glycol conformers as a function of draw ratio were thus generated. At a given λ, the proportion of *gauche* glycol conformers along each chain sampled in the network calculations was recorded and averaged over the MC sample of chains.

3.3. Orientation of a segment vector in a deformed network

In the MC scheme, at each value of λ, the average orientation function of segments in chain i of the MC sample relative to its end-to-end vector, $\langle P_2(\cos\xi)\rangle_i$, is found (see Fig. 5). The end-to-end vector orientation for chain i relative to the draw direction $P_2(\cos\psi_i)$ is also found and the average segment orientation for chain i relative to the draw direction is calculated using the Legendre addition theorem [10].

$$\langle P_2(\cos\zeta)\rangle_i = \langle P_2(\cos\psi_i)\langle P_2(\cos\xi)\rangle_i\rangle. \tag{12}$$

The average segmental orientation relative to the draw direction over the whole MC sample of N chains is then found with

$$\langle P_2(\cos\zeta)\rangle = \sum_{i=1}^{N}\langle P_2(\cos\zeta)\rangle_i/N. \tag{13}$$

In the present work, $\langle P_2(\cos\zeta_{ter})\rangle$ was evaluated for the terephthaloyl segments.

4. Results and discussion

The densities of the drawn PET films at various draw ratios are plotted in Fig. 6. It can be seen that there is a rapid increase in the density for draw ratios above 2, consistent with the onset of crystallisation at $\lambda \sim 2.5$ seen previously [30].

The experimentally measured and theoretically predicted values of the *gauche* content of the glycol segment are plotted in Fig. 7 as functions of the draw ratio. The experimental *gauche* content of 76% at zero deformation was predicted by the new RIS model for the PET chain at 541 K with $E_{\sigma 5} = 4.16$ kJ mol^{-1}. The temperature of 541 K is consistent with the melt temperature of 533–553 K. The calculated points in Fig. 7 actually refer to 523 K, the temperature for which the samples of chain conformations were generated when the new RIS model was established. The change of temperature from 541 to 523 K has a negligible effect on the calculated properties to be discussed in this and the following papers. For example, the glycol *gauche* content at 523 K and zero deformation lies between 76.5% and 76.0%.

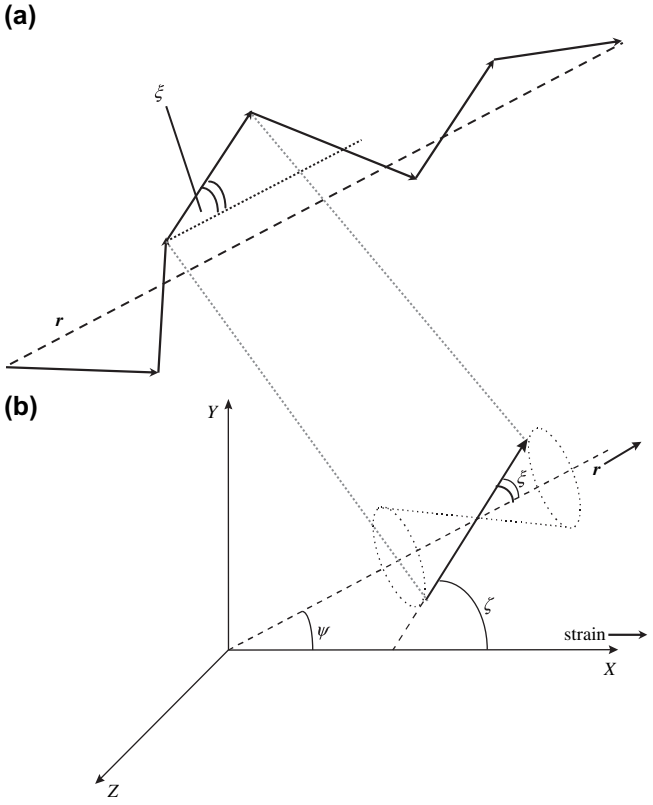

Fig. 5. (a) Illustration of the orientation angle ξ between a segment vector and the chain vector, $\boldsymbol{r}$. (b) Illustration of orientation angles: ξ, between a segment vector and $\boldsymbol{r}$; ψ, between $\boldsymbol{r}$ and the uniaxial strain direction; and ζ, the angle between a segment vector and the strain direction. The segment is assumed to randomly occupy all positions on the cone defined by ξ, so that the calculated value of $\langle P_2(\cos\zeta)\rangle$ is an average, sampled over all cone positions of ξ.

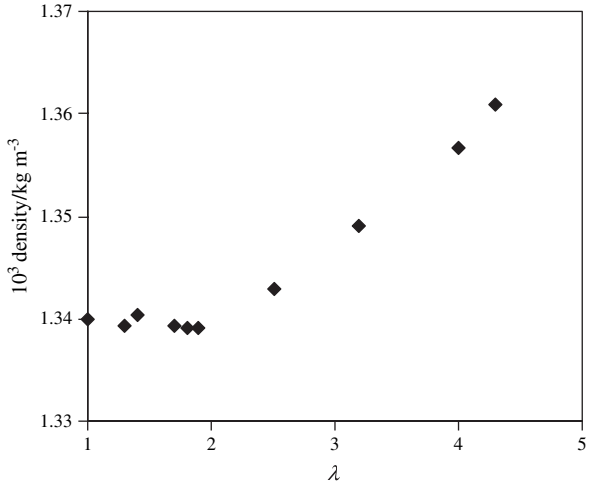

Fig. 6. Densities of the drawn PET films at 298 K as a function of draw ratio, λ.

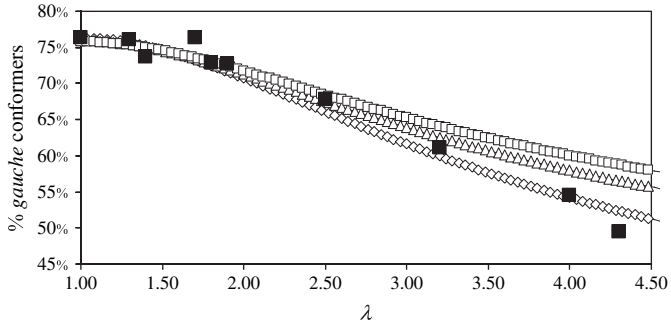

Fig. 7. Experimentally measured values of *gauche* content as a function of the draw ratio λ (■), compared with theoretically predicted values for networks of 9 (◇), 10 (△) and 11 (□) repeat units per chain at 523 K.

The modelling results in Fig. 7 show that, at a given value of λ, the *gauche* content decreases as chain length decreases, indicating that the average chain extension is greater for shorter chains. It can be seen that for low draw ratios the experimental data most closely match the theoretical curves generated for $n = 10$. Above $\lambda = 2.5$ the measured *gauche* content decreases below that predicted. It should be remembered that the predictions are for independent chain behaviour. Hence, it would appear that the onset of crystallisation causes a larger increase in *trans* content consistent with a greater extension of the glycol segments.

Fig. 8 shows the values of the orientation of the terephthaloyl segment obtained from the sets of infra-red absorption bands described in Fig. 3. It can be seen that there is reasonable agreement between the results from the in-plane and out-of-plane absorbances, with some experimental scatter at the lower values of $\langle P_2(\cos\zeta_{ter})\rangle$. The two values of $\langle P_2(\cos\zeta_{ter})\rangle$ obtained at each λ were averaged and a least-squares fit performed on the data. These averaged experimental results are plotted in Fig. 9, together with the theoretically predicted values. The

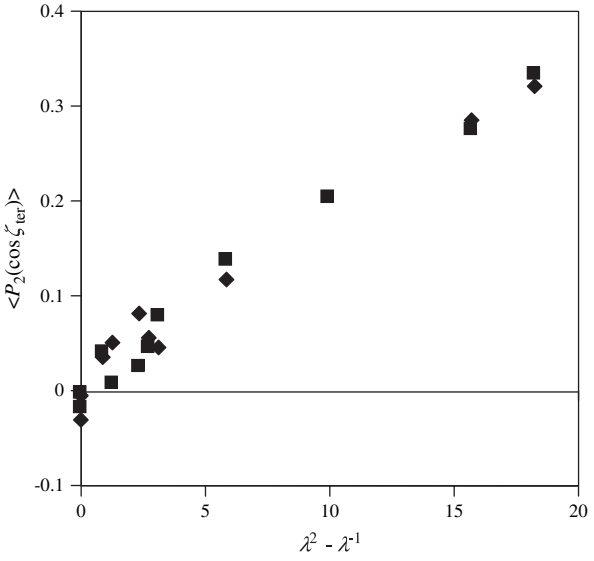

Fig. 8. Average orientation of the terephthaloyl segments determined from measurements of the infra-red absorbance bands defined in Fig. 3, due to in-plane vibrations (parallel to the segment axis) (◆) and out-of-plane vibrations (perpendicular to the segment axis) (■).

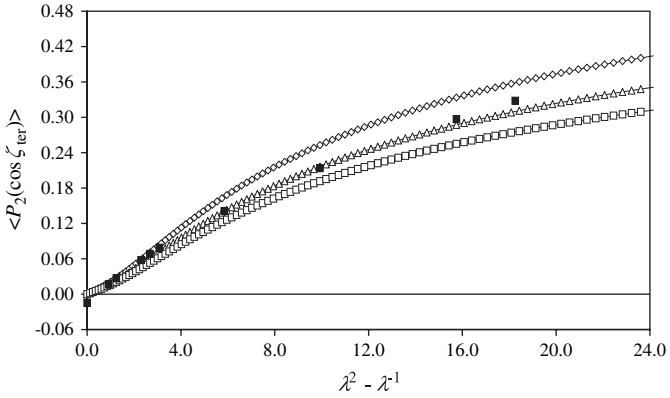

Fig. 9. Average experimental values of the terephthaloyl segment orientation as a function of $\lambda^2 - \lambda^{-1}$ (■), compared with theoretically predicted values for networks of 9 (◇), 10 (△) and 11 (□) repeat units per chain at 523 K.

modelling shows that $\langle P_2(\cos\zeta_{ter})\rangle$ is not linearly related to $\lambda^2 - \lambda^{-1}$ and that, consistent with the results on the populations of glycol conformers, orientation increases as chain length decreases. Again the experimental data most closely match the curve generated for $n = 10$, and in this case the onset of crystallisation does not initially appear to affect the agreement between the experimentally measured and theoretically predicted values.

5. Conclusions

It has been shown that the experimental data for PET films for the change in *gauche* glycol content and the development of terephthaloyl group orientation are both consistent with the theoretical predictions for the deformation of a PET network with about 10 monomer units per chain. It should be noted that M_n of the parent chain is 19,500 corresponding to about 100 repeat units. Thus, there were about 10 entanglement network chains per parent chain. The results provide excellent confirmation of the RIS Monte Carlo modelling of Stepto and collaborators [8–10]. In the following papers, the modelling will be applied to the prediction and interpretation of the stress–optical, strain–optical and stress–strain properties of PET.

Acknowledgement

The authors gratefully acknowledge the financial support of the EPSRC.

References

[1] Pinnock PR, Ward IM. Trans Faraday Soc 1966;62:1308.
[2] Long SD, Ward IM. J Appl Polym Sci 1991;42:1911.
[3] Cunningham A, Ward IM, Willis HA, Zichy V. Polymer 1974;15:749.
[4] Purvis J, Bower DI, Ward IM. Polymer 1973;14:398.
[5] Nobbs JH, Bower DI, Ward IM. J Polym Sci Polym Phys Ed 1979; 17:259.
[6] Ward IM. Adv Polym Sci 1985;66:81.
[7] Kuhn W, Grun F. Kolloid Z 1942;101:248.
[8] Stepto RFT, Taylor DJR. Macromol Symp 1995;93:261.

[9] Stepto RFT, Taylor DJR. J Chem Soc Faraday Trans 1995;91:2639.
[10] Taylor DJR, Stepto RFT, Jones RA, Ward IM. Macromolecules 1999; 32:1978.
[11] Ward IM, Bleackley M, Taylor DJR, Cail JI, Stepto RFT. Polym Eng Sci 1999;39:2335.
[12] Cail JI, Stepto RFT, Taylor DJR, Jones RA, Ward IM. Phys Chem Chem Phys 2000;2:4361.
[13] Saunders LS, Ward IM, Cail JI, Stepto RFT. Polymer 2004;45:2357.
[14] Cail JI, Stepto RFT. Polymer 2003;44:6077.
[15] DuPont UK, private communication.
[16] Ravens DAS, Ward IM. Trans Faraday Soc 1961;57:150.
[17] Yazdanian M, Ward IM, Brody H. Polymer 1985;26:1779.
[18] Hutchinson IJ, Ward IM, Willis HA, Zichy V. Polymer 1980;21:55.
[19] Spiby P. Ph.D., University of Leeds; 1988.
[20] Green DI, Bower DI. Spectrochim Acta A – Mol Biomol Spectrosc 1993;49:1191.
[21] Thermo Galactic, 395 Main Street, Salem, NH 03079, USA.
[22] Cunningham A, Davies GR, Ward IM. Polymer 1974;15:743.
[23] Ward IM. Chem Ind 1956;905.
[24] Ward IM. Chem Ind 1957;1102.
[25] Grime D, Ward IM. Trans Faraday Soc 1958;54:959.
[26] Ward IM, Wilding MA. Polymer 1977;18:327.
[27] Boerio FJ, Bahl SK, McGrew GE. J Polym Sci Polym Phys Ed 1976; 14:1029.
[28] Williams AD, Flory PJ. J Polym Sci A2 1967;5:417.
[29] Cail JI, Stepto RFT, Ward IM. Polymer 2007;48:1367.
[30] Middleton AC, Duckett RA, Ward IM, Mahendrasingam A, Martin C. J Appl Polym Sci 2001;79:1825.